Construction and Building Materials 363 (2023) 129715

Contents lists available at ScienceDirect

Construction and Building Materials

journal homepage: www.elsevier.com/locate/conbuildmat

The effect of waste marble and basalt aggregates on the fresh and hardened properties of high strength self-compacting concrete

Ahmet Raif Boğa [a,*], Ahmet Ferdi Şenol [b]

[a] Afyon Kocatepe University, Faculty of Engineering, Civil Engineering Department, 03200 Afyonkarahisar, Turkey
[b] Bilecik Seyh Edebali University, Faculty of Engineering, Civil Engineering Department, 11100 Bilecik, Turkey

ARTICLE INFO

Keywords:
High strength self-compacting concrete
Waste marble aggregate
Basalt aggregate
Silica fume
Microstructure
Interface transition zones

ABSTRACT

With the increase in concrete production worldwide in recent years, our natural aggregate resources are rapidly depleting. Various waste aggregates are used as an alternative to natural aggregates to solve this problem. However, the demand for High Strength Self-Compacting Concrete (HSSCC) in the concrete industry is increasing. Using waste aggregates as coarse aggregate in HSSCCs may increase the sustainability of HSSCCs, while simultaneously reducing environmental waste problems and production costs. This study aims to produce the HSSCC series by using basalt and waste marble aggregates in certain volumetric ratios instead of limestone-based crushed stone used as coarse aggregate in concrete production. To achieve this aim, the effect of aggregate type was investigated on the physical, mechanical, and durability properties of the produced concrete series. In the production of HSSCC series, silica fume and cement were used in fixed proportions. Instead of limestone-based coarse aggregates, waste marble and basalt aggregates were used at 25, 50, 75, and 100 % ratios by volume. Thus, a series of eight different HSSCCs and a control HSSCC were created. Slump flow, T_{500} time, V-funnel, and L-box tests were applied to assess the flowability, filling, and passing ability of the produced HSSCC series. Cylindrical specimens of 100 × 200 mm and cubes of 150 × 150 × 150 mm were produced with the prepared mixture series. The produced specimens were subjected to standard curing for 28 and 180 days in lime-saturated water pools with a temperature of 20 ± 2 ℃. After the curing period, ultrasonic pulse velocity, compressive strength, splitting-tensile strength, apparent porosity, sorptivity, rapid chloride permeability, electrical resistivity tests, and internal structure analyzes were applied to the specimens. According to the fresh concrete test results, no segregation was observed in all of the HSSCC series and it was observed that they were in compliance with the fresh state standards. When 180-day curing was applied to the HSSCC series, the compressive strength of the series in which 25 % waste marble aggregate was used increased by 9.1 % compared to the control series, while the compressive strength of the series in which 100 % basalt aggregate was used increased by 19.5 %. As a result, it has been observed that HSSCCs with high strength and durability properties can be produced by using basalt or waste marble aggregates at rates of 25 % to 100 % instead of crushed stone aggregates.

1. Introduction

In the construction industry, the use of high-performance concretes is increasing day by day in the construction of complex structures with significant heights and spans (such as skyscrapers, high towers, and large bridges) [1]. This is due to improvements in structural performance, such as the higher strength and durability that high-strength concrete will provide, compared to conventional normal strength concrete [2]. Concretes are defined as normal strength (20 to 50 MPa), high strength (50 to 120 MPa), ultra-high strength (over 120 MPa), conventional and high-performance concretes [3].

Self-Compacting Concrete (SCC), which was first designed by H. Okamura in 1986 to produce durable concrete, was first used in practical constructions in Japan and mostly in large construction companies [4]. Continuing to increase its usage area in recent years, SCC is defined as an innovative concrete that is not exposed to external influences and can be easily placed in the mold in which it is poured without creating a void [5,6]. SCC is the most suitable option for beam-column junction and densely-reinforced structural members of bridges and foundations [7]. The structures to be built with the combination of high strength and self-

* Corresponding author.
E-mail address: araif@aku.edu.tr (A. Raif Boğa).

https://doi.org/10.1016/j.conbuildmat.2022.129715
Received 19 August 2022; Received in revised form 6 November 2022; Accepted 7 November 2022
Available online 13 December 2022

compacting technology will become more durable compared to conventional method concretes [8]. Considering the advantages of using SCC, it is considered that High Strength Self-Compacting Concrete (HSSCC) will be preferred more because of the expected performance from members in high-rise buildings (especially on lower floors) [9].

The consumption of natural aggregates, which constitutes approximately 70–80 % of the concrete volume, is increasing rapidly with the increase in concrete production and use[10]. As it is known, the amount of aggregate to be used in the concrete mixture will also affect the low cost of the concrete. For this purpose, researchers are working on the use of waste aggregate, which will prevent the depletion of our natural aggregate resources and contribute to the production of concrete in terms of economy and durability.

Basalt used as concrete aggregate has different colors such as dark, gray, and dark grayish. Basalt usually contains 45–52 % silica (SiO_2) and oxides such as iron, calcium, and magnesium, compared to the most common igneous rocks [11]. Basaltic rocks' crushing and cohesive strengths are 170–220 MPa and 32–44 MPa, respectively [12]. Basalt aggregates are used in many countries, especially in the construction of road and airport pavements. The fact that basalt aggregates have high specific gravity and lower water absorption and wear loss values proves that it is suitable for use in concrete production [13]. Sarireh [14] conducted a study using basalt aggregates compared to crushed limestone and rounded valley aggregate concrete to produce high-strength and durable concrete. It was determined that in the mixtures prepared for different concrete qualities, there was a 15–40 % increase in compressive strength and a 35–50 % improvement in tensile strength using basalt aggregate.

Marble constitutes 50 % of the natural stone production in the world [15]. According to the statistical results in the Natural Stones Sector Report [16] prepared by the Ministry of Commerce of the Republic of Turkey, Turkey is one of the top 5 countries that produce and export the most natural stones in the world between the years 2018–2020. Marble production comes first with a share of 95 % of total natural stone exports in Turkey. This large marble production industry produces large amounts of marble waste [17–19]. The wastes in marble processing plants are generally in the form of marble sludge and broken marble pieces. These wastes, which create various environmental problems in nature, are being disposed to open lands (Fig. 1). Marble waste, which poses a threat to the environment, also has some advantages that reduce the total void content when used as a cement or aggregate substitute in concrete and pavement[20].

Researchers have conducted some studies on the use of marble waste in conventional concrete and SCCs. However, most of the studies use waste marble as fine aggregate or cement substitute in conventional concrete and normal strength SCC [21–26]. Vaidevi et al. [27] produced SCCs using 0, 25, 50, and 100 % by weight marble waste instead of fine aggregate in concrete. Mechanical and chemical tests such as compressive, flexure, and splitting tensile strengths and acid and sulfate attack were applied to SCC specimens at 28 and 56 days of age. As a result of the study, it was determined that the use of waste marble aggregate up to 25 % instead of fine aggregate in SCC increased the strength and durability compared to the control SCC. Sadek et al. [28] investigated the use of marble and granite powders as mineral additives in SCC. They produced different SCC series by replacing the cement volume in the control series with marble or granite powders at 20, 30, 40, and 50 % by ratios. As a result of the study, it was concluded that waste marble and granite powders can be used up to 50 % of the cement volume in SCCs and that the performance of granite powder in concrete is higher than marble powder. Andre et al. [29], produced different concrete series by substituting the coarse aggregate ratios in three different normal concrete series consisting of coarse aggregates such as limestone, granite, and basalt with marble aggregates. They have replaced each coarse aggregate volume in the concrete series with marble aggregate at 20, 50, and 100 % ratios. At the end of the study, they determined that the concrete created with the use of marble aggregate; has similar properties in terms of durability compared to the concrete formed with coarse aggregates such as limestone, granite, and basalt and that marble aggregates can be applied by including them in the concrete. Choudhary et al. [30] prepared 16 HSSCC mixtures in binary, ternary, and quaternary form by adding marble waste dust, fly ash, and silica fume instead of cement and a control mixture containing only cement as a binder. As a result of the study, they found that the incorporation of marble waste and fly ash into the mixture improves the fresh properties of high-strength SCCs. It was concluded that the use of 10 % marble waste dust, 15 % fly ash, and 5 % silica fume as cement substitutes in the mixtures reached the optimum mechanical performance. Kore and Vyas [18], investigated the use of marble waste as coarse aggregate in conventional concrete. They replaced the traditional natural coarse aggregate with marble aggregate at 0–100 % by weight. As a result of the study, they stated that the workability increased with the increase in the use of marble aggregate, and this was due to the low water absorption and flat smooth surface properties of the marble aggregate. In their experiments on the hardened concrete series on the 7th and 28th days, they concluded that the average compressive strength of the series increased by 40 % and 18 %, respectively. Srikanth et al. [31], instead of traditional coarse aggregate in the mixtures; produced four different concrete series and a control series concrete by using 100 % waste

Fig. 1. Marble waste dumped in open lands.

granite marble chips, angular aggregate, demolished aggregate and round aggregates. According to the compressive strength results of the concrete series at the end of the 28th day, they found that concrete produced using waste granite marble chips was the best alternative to conventional coarse aggregate, and the round aggregate concrete series gave the lowest results. The number of studies on the use of marble waste as a coarse aggregate substitute in SCCs is very few. Uygunoğlu et al. [32] investigated the use of recycled aggregate obtained from 100 % marble waste and crushed concrete instead of limestone aggregate in SCC production. As a result of the study, they determined that the workability properties of SCC, such as flowability, blocking resistance, and segregation resistance, could be increased by using marble waste. In addition, as a result of the experiments, they stated that the use of marble waste and recycled aggregate did not cause significant differences in the mechanical properties of SCC, and these aggregates could be used in SCC.

Many studies in recent years have investigated the use of marble waste as a partial substitute for concrete component materials. However, the number of studies investigating the effects of the use of marble waste as a coarse aggregate substitute in high-strength SCCs on mechanical, rheological, microstructure, and durability properties is limited. In addition, the comparison of waste marble aggregates used as coarse aggregate replacement in high-strength SCCs with the performances of other aggregate types has not been fully investigated. However, the majority of SCC studies with waste marble aggregate are based on short-term curing age. The use of waste marble aggregates as coarse aggregate in SCC can always create uncertainty and raise concerns about mechanical and durability properties. In this study, it was aimed to examine the physical, mechanical, durability, and micro-structural properties of high-strength SCC series produced by the use of waste marble aggregates as coarse aggregate, especially in advanced ages (180 days). In addition, another aim of the study is to produce sustainable HSSCCs by substituting basalt and waste marble aggregates in high volume ratios instead of limestone-based crushed stone aggregate. Thus, it is considered that the use of waste marble aggregates as coarse aggregate in HSSCC production will be an alternative to natural aggregate resources and will also benefit from reducing environmental waste problems. For this purpose, eight different HSSCC series and a control HSSCC were created by using waste marble and basalt aggregates instead of limestone-based aggregates at 25, 50, 75 and 100 % by volume. After the productions, first of all, the fresh properties of the HSSCC series were determined, and ultrasonic pulse velocity, compressive strength, splitting-tensile strength, apparent porosity, sorptivity, rapid chloride permeability and electrical resistivity tests were applied on the hardened specimens. Finally, the microstructural properties of concrete were investigated using Scanning Electron Microscopy (SEM). As a result of the experiments, the usability of the basalt aggregate, which is common in nature, and the marble aggregates obtained from the waste marble fields, in HSSCC were examined comparatively.

2. Experimental study

The production process and applied experiments of HSCCC series are shown in the flow chart in Fig. 2.

2.1. Materials used

In the production of HSSCC, CEM I 52.5 N Portland Cement in accordance with TS EN 197–1[33], produced by ÇİMSA Afyon Cement Factory, and silica fume (SF), which is the waste of Antalya Eti Elektrometalurji A.Ş. were used. In the mixtures, limestone-based crushed sand (0–4 mm) and crushed stone I (4–11.2 mm) aggregates obtained

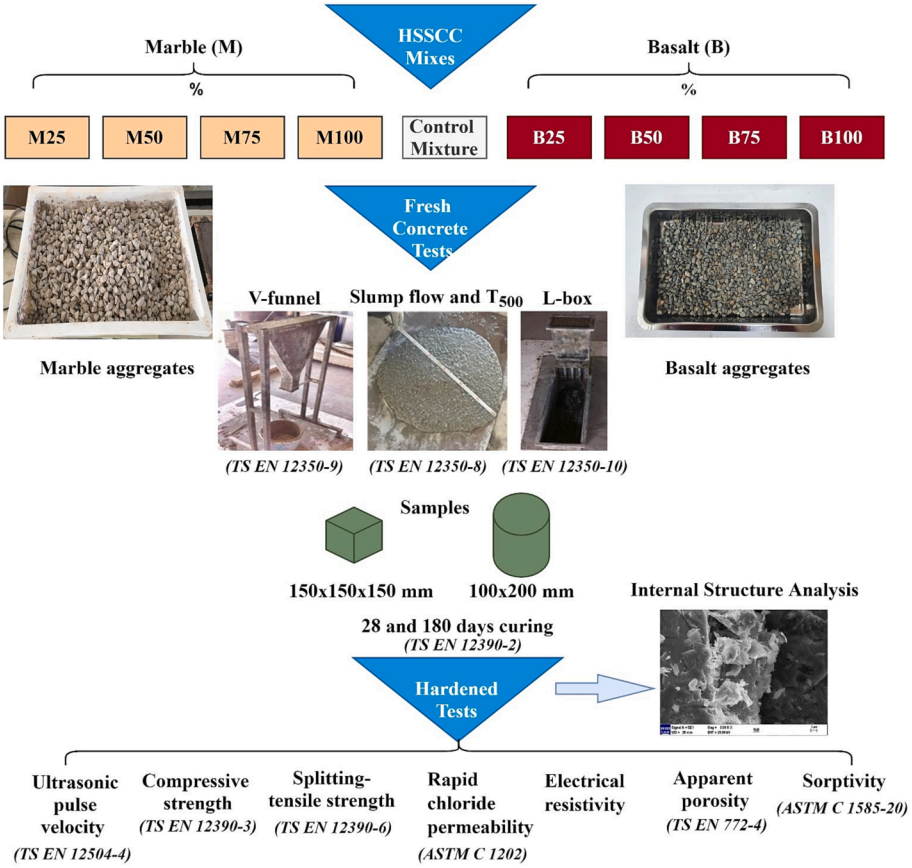

Fig. 2. Flowchart of the mixing and testing procedures.

from the quarries of Afyon KOLSAN ready-mixed concrete facility were used. The results of XRF analysis on cement and silica fume specimens used in the mixtures are given in Table 1.

Waste marble (M) aggregates used in HSSCC production was obtained from SAY Yapı A.Ş, which collects marble waste in Afyonkarahisar Province Organized Industrial Zone, and basalt (B) aggregates were obtained from the province of Kütahya. The grain sizes of the M (Fig. 3) and B aggregates used in the mixtures are in the range of 4–11.2 mm. The specific gravity of M and B aggregates are 2.55 and 2.64, respectively, and their water absorption percentages are 0.692 and 1.13. In addition, XRF analysis results of powder specimens obtained from aggregates used in HSSCC production are shown in Table 2.

The specific gravity of sand and crushed stone I (limestone) aggregates are 2.657 and 2.698, respectively, and their water absorption percentages are 1.276 and 0.689. Sieve analysis was carried out on the aggregates, and to compare the granulometry curves of waste marble, basalt, crushed stone I aggregate, and crushed sand are given together in Fig. 4. As seen in Fig. 4, the granulometry curves of M, B, and crushed stone I aggregates overlapped. In other words, the particle distributions of the aggregates used in 4–11.2 mm sizes are very close to each other. In HSSCC productions, crushed sand and crushed stone I aggregates were used at 50 % and 50 % by volume, respectively. By replacing the M and B aggregates with the crushed stone I aggregate at 25, 50, 75, and 100 % volumetric ratios, HSSCC series with M and B aggregates were obtained.

Los Angeles abrasion (LA) [34], aggregate impact value (AIV) [35], aggregate crushing value (ACV) [36] and uniaxial compressive strength (UCS) [37] tests were performed on the aggregates. The results obtained from the tests on aggregates are shown in Table 3. When Table 3 was examined, better results were obtained from basalt aggregate compared to other aggregates. The values obtained from limestone and waste marble aggregate are quite similar. When the LA and ACV values were examined, it was observed that these values were very close to each other in all three aggregates. In the study of Kamani and Ajalloeian [38], LA and ACV values are similar to each other. Polycarboxylic ether-based Basf Ace 450 with hyperplasticizer (HP) concrete admixture between 0.85 and 1% of the binder material was used to ensure workability in HSSCC productions.

Table 1
Properties of Portland cement and silica fume.

	Components, %	CEM I 52.5 N	SF
Chemical properties (XRF)	SiO_2	19.96	80.22
	Al_2O_3	5.44	0.84
	Fe_2O_3	3.25	0.46
	CaO	63.98	1.39
	MgO	1.64	6.55
	Na_2O	0.17	1.45
	K_2O	0.45	2.23
	SO_3	2.98	1.04
	ZnO	–	0.26
	MnO	–	–
	Cr_2O_3	–	1.69
	Cl^-	0.0060	0.027
	F	–	0.27
	Loss on ignition	1.94	3.35
	Insoluble residue	0.15	–
	Free CaO	1.10	–
Physical properties	Specific gravity	3.12	2.20
	Specific surface, cm^2/g	5012	–
	BET, m^2/g	–	13.02
	Initial setting time, min	110	–
	Final setting time, min	157	–
	Volume expansion, mm	0	–
Compressive strength	2 days, MPa	36.2	–
	7 days, MPa	52.4	–
	28 days, MPa	64.7	–

2.2. Mix proportioning

HSSCCs were designed according to EFNARC [5] standards by using 25, 50, 75, and 100 % by volume M and B aggregates instead of the limestone-based crushed stone I aggregate (4–11.2 mm) used in the control (C) mixture. M and B indices in the names of the designed concrete mixtures represent waste marble and basalt aggregates, respectively. M25, M50, M75, and M100 indices indicate that the concrete series contain 25, 50, 75, and 100 % waste marble aggregates by volume; B25, B50, B75, and B100 indices show that the concrete series contain basalt aggregates at 25, 50, 75 and 100 % by volume. Since the aggregates of crushed-stone I, M and B have different specific weights, the aggregates have been displaced by volume in the mixtures. In HSSCC production, according to EFNARC [5] criteria, a high percentage of powdered material (400–600 kg/m^3) should be used to provide fresh properties. In the study, a total of 500 kg/m^3 powder material was used. The water/powder material ratio was chosen as 0.35. If only cement is used as powder material in self-compacting concrete designs, the concrete produced will not be economical and sustainable. The fact that the production of cemented concrete consumes our natural resources and causes high CO_2 emissions from cement creates negative effects on the environment. Therefore, the use of waste materials such as silica fume in concrete will contribute to sustainable green concrete production in order to reduce these negative effects caused by cementitious concrete production in recent years. Reducing the amount of cement is a very critical and economic situation for sustainability. However, it should be noted that silica fume increases the cost of cement due to the higher price of the fume compared to cement and the need for higher amounts of admixtures.

Typically, the SiO_2 content in the SF is expected to be above 85 %. SF containing a lower percentage of SiO_2 is less pozzolanic [39]. The SiO_2 ratio of silica fume used in the study is around 80 %. For this reason, high rates of silica fume were used in order to contribute to the pozzolanic reactions and to benefit from the filling effect.

Replacing cement with high doses (5–20 %) of SF causes a significant increase in the mechanical properties and durability performance of concrete. The addition of SF to the concrete mix increases the water demand due to its high surface area. Water-reducing admixtures are widely used to maintain the desired workability at a desired water/cement ratio [39]. In the study, the desired workability properties were provided.

While designing the mixture, the typical ranges by mass and volume of the constituents given in EFNARC [5] and TS 802 [40] standards were used. In the study, powder: 500 kg/m^3, paste volume: 379 L/m^3, water: 175 L/m^3, coarse aggregate: 837 kg/m^3, coarse aggregate volume: 310 L/m^3, water/powder ratio by volume: 0.97. All values fall between the limit values given in EFNARC [5] and TS 802 [40]. The amount of admixture was used in such a way as to ensure self-compacting without causing any segregation in the mixtures. The mixture ratios obtained are given in Table 4.

2.3. Specimen types produced and curing

After the mixing ratios were determined, concrete casting processes were carried out. The fresh concrete mixes produced were placed in Φ100 × 200 mm cylindrical and 150 × 150 × 150 mm cube specimen molds. Three cube and cylindrical specimens were produced for each series, and the concrete specimens in the molds were kept in the laboratory for 24 h and then removed from their molds. Standard curing was applied to the produced HSSCC specimens in lime-saturated water pools with a temperature of 20 ± 2 °C until the 28th and 180th days, and then the relevant experiments were conducted. The HSSCC series poured into molds and cured are shown in Fig. 5. Ultrasonic pulse velocity and compressive strength tests were carried out on cube specimens, and splitting-tensile strength, apparent porosity, sorptivity, rapid chloride permeability and electrical resistivity tests were performed on

Fig. 3. Waste marble aggregates.

Table 2
Chemical analysis results of aggregate specimens.

Oxide components	Waste marble (%)	Basalt (%)	Limestone (%)
Na_2O	0.06	2.34	0.03
MgO	1.37	4.12	1.63
Al_2O_3	1.08	16.12	0.82
SiO_2	0.18	50.57	1.72
P_2O_5	–	0.37	–
SO_3	0.06	0.08	0.02
Cl	0.03	–	0.01
K_2O	0.02	2.27	0.08
CaO	54.10	9.76	52.50
TiO_2	–	0.94	–
MnO	–	0.19	0.01
Fe_2O_3	0.08	9.02	0.15
SrO	–	0.15	–
BaO	–	0.16	–
Loss of ignition	43.00	3.42	42.90

cylindrical specimens.

2.4. Tests

2.4.1. Fresh and hardened concrete tests

To determine the fresh properties of HSSCCs, slump flow test and T_{500} time [41], V-Funnel [42], and L-Box [43] tests were applied on the mixtures. In order to determine the mechanical properties of HSSCCs, hardened concrete tests were applied to the specimens prepared in TS EN 12390–1 [44] and TS 12390–2 [45] standards. Sectional views of the HSSCC series with basalt and waste marble aggregate are shown in Figs. 6 and 7.

Ultrasonic pulse velocity tests were carried out on cube specimens of 150 × 150 × 150 mm, after 28 and 180 days of standard curing, in accordance with TS EN 12504–4[46]. Then, compressive strength tests were carried out on the same specimens in accordance with TS EN 12390–3[47]. Splitting-tensile strength tests were carried out on Φ100 × 200 mm cylindrical specimens after 28 and 180 days of standard curing, according to TS EN 12390–6 [48].

The durability properties of concrete were determined in accordance with ASTM C 1202[49]. In the rapid chloride permeability experiments,

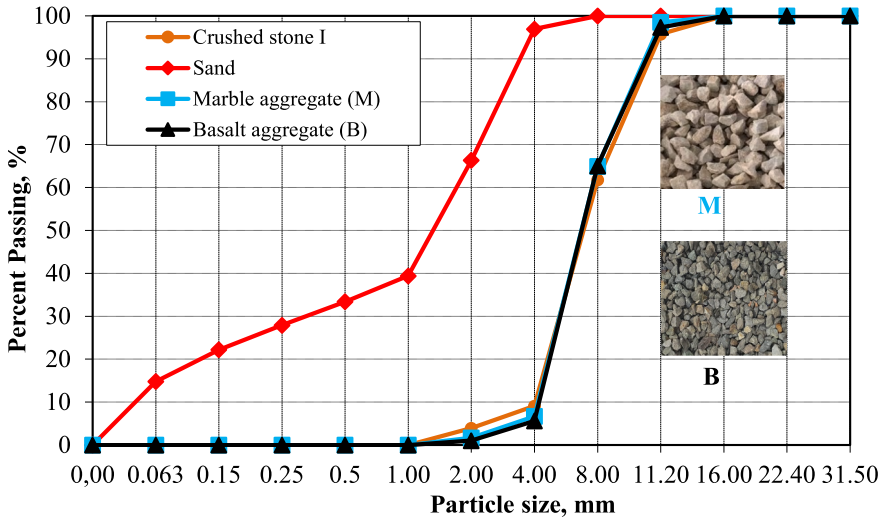

Fig. 4. The granulometry curves of all aggregates used.

Table 3
Test results of the aggregates.

Test name		Standards	Aggregates		
			Basalt	Limestone	Waste Marble
Los Angeles Abrasion Value (LA), %		TS EN 1097–2 [34]	16.45	24.15	24.94
Aggregate Impact Value (AIV), %		BS 812–112 [35]	5.10	11.54	13.65
Aggregate Crushing Value (ACV), %		BS 812–110 [36]	14.29	22.95	23.58
Uniaxial Compressive Strength (UCS), MPa		TS EN 1926 [37]	144	113	109

disc-shaped specimens of Φ100x50 mm, obtained by cutting Φ100 × 200 mm cylindrical specimens, were used. Before this experiment, 28 and 180 days standard curing was applied to the specimens. Before the rapid chloride permeability test, the specimens were vacuumed according to ASTM C 1202[49]. The preparation of the specimens for the experiment with the vacuum pump and the rapid chloride permeability test setup are shown in Fig. 8.

At the end of the 6 h, the total charge passed of specimens placed in the rapid chloride permeability test setup were determined. The rapid chloride permeability levels of the produced HSSCCs were determined by comparing the total charge passed values obtained as a result of the experiments with the ASTM C 1202 limit values given in Table 5.

Electrical resistivity tests were performed on Φ100x200 mm cylindrical specimens after 28 and 180 days of standard curing. Before the electrical resistivity measurements, the specimens were saturated with water. Table 6 was used to evaluate the relationships between electrical

Table 4
The mixing ratios of the HSSCC series (kg/m^3).

Mixes	Water	Cement	Silica fume	Crushed sand (0–4 mm)	Crushed stone I (4–11.2 mm)	Marble (M)	Basalt (B)	HP
C	175	350	150	824	837	-	-	4.50
M25	175	350	150	825	628	198	–	4.25
M50	175	350	150	825	419	396	–	4.25
M75	175	350	150	825	209	594	–	4.25
M100	175	350	150	824	–	791	–	4.40
B25	175	350	150	825	628	–	205	4.30
B50	175	350	150	824	419	–	410	4.50
B75	175	350	150	824	209	–	614	4.75
B100	175	350	150	824	–	–	818	5.00

Fig. 5. Molded and cured HSSCC series.

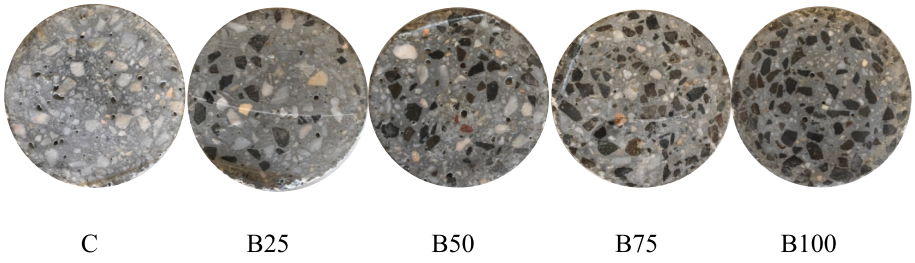

Fig. 6. Cross-sectional views of HSCCC series with basalt aggregate.

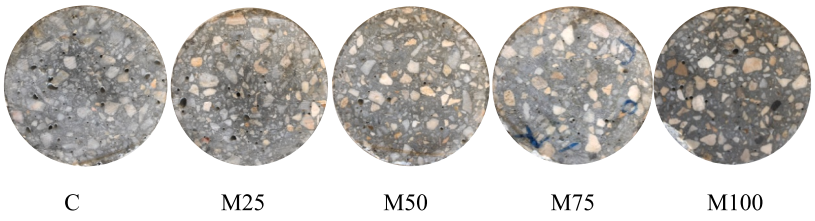

Fig. 7. Cross-sectional views of HSSCC series with waste marble aggregate.

resistivity and corrosion probability.

In order to calculate the sorptivity coefficient and the apparent porosity percentages, Φ100x200 mm cylindrical specimens were produced. The produced cylindrical specimens were cured for 28 and 180 days. Archimedes balance was used to determine the weights of the specimens in water, and the apparent porosity values of the HSSCC series were calculated using Equation (1) [51].

Apparent porosity (AP) (%) = $((W_d\text{-}W_o)/(W_d\text{-}W_s))x100$ (1).

In Equation (1); W_o: the weight of the specimen dried at 105 ℃ for 24 h (g), W_s: the saturated weight of the specimen in water (g), W_d: the weight of the specimen at the saturated condition in the air (g), AP: the apparent porosity value (%).

Before the sorptivity tests, the specimens were dried in an oven for 24 h, and then the sorptivity tests were carried out. The sorptivity coefficient (k) values were calculated with the help of Equation (2) and Equation (3).

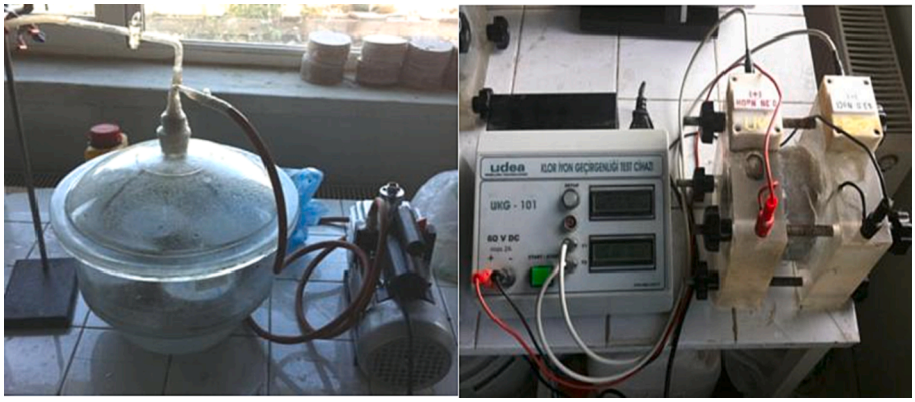

Fig. 8. Vacuum treatment and rapid chloride permeability test setup.

Table 5
ASTM C 1202 limit values.

Total charge passed (Coulmb)	Permeability
>4000	High
4000–2000	Moderate
2000–1000	Low
1000–100	Very low
<100	Negligible

Table 6
Relationship between electrical resistivity and corrosion probability[50].

Electrical resistivity (kΩ.cm)	Corrosion probability
<5	Very high
5–10	High
10–20	Low
>20	Negligible

$q^2 = k \times t$ (2)

$q^2 = (Q/A)^2$ (3).

In equations; Q: The amount of water absorbed by the specimen (g), A: the area of the water-impregnated surface (cm^2), q: the amount of water absorbed per unit area (g/cm^2), t: the water absorption time of the specimen (*sec*).

Pieces were taken from the 180-day standard cured specimens of the HSSCC series, and internal structure images were taken with Zeiss LEO1430VP brand scanning electron microscope (SEM), and analyzed.

3. Evaluation of test results

3.1. Fresh concrete test results

According to the fresh concrete test results, no segregation was observed in all of the HSSCC series and it was observed that they were in compliance with the fresh state standards determined by TS EN 206 + A2 [52]. The results of the flow diameter, T_{500} time, V-funnel flow time and L-box experiments of fresh HSSCC mixtures are given in Fig. 9. The fresh properties of the HSSCC series were evaluated according to the limit values recommended by TS EN 206 + A2 [52] and the class they belonged to was determined. As can be seen from Table 4, the amounts of hyperplasticizer (HP) admixtures were not used at a fixed rate in the study. The aim of the study is to produce HSSCC series with similar workability properties. For this, slump flow values are intended to be in SF1 (550–650 mm) class and T_{500} values in VS1 (<2.0 *sec*) class. HP admixture amounts have been adjusted in a controlled manner. After providing these workability classes, V-funnel and L-box experiments were also carried out.

When Fig. 9 is examined, it has been determined that the flow diameter results vary between 575 and 670 mm and all series except B100 series are in the SF1 (550 to 650 mm) class. The highest flow diameter result (670 mm) in the HSSCC series was observed in the B100 series. According to the T_{500} time results of fresh HSSCCs, all series reached a diameter of 500 mm in under 2 s (1.20–1.90 *sec*.). That's why all HSSCC series are in VS1 class. In general, higher T_{500} times were obtained in series with smaller flow diameters. The V-funnel flow time values obtained from the HSSCC series were between 2.38 and 4.23 *sec*, with all values below 9.0 *sec*. Thus, it has been concluded that the produced HSSCC series are in the VF1 class. Generally, the series with a high spreading time to 500 mm diameter also had high V-funnel flow times. L-box test results (h_2/h_1 ratios) ranged from 0.80 to 0.93. Thus, all series are in PL2 class and have reached the ability to pass through dense reinforcements without obstruction.

As can be seen from Fig. 9a, flow diameter of 600 mm was obtained in the control series. When the same amount of admixtures as the control series was used in the pilot casting made with marble aggregate, it was decided to reduce the amount of admixtures used, since segregation was observed in these series. As can be seen from Table 4, by using fewer admixtures from the control series, the tendency to segregation was prevented, and M25, M50, and M75 series were produced in SF1 class. It is thought that the observation of segregation tendencies when similar admixtures are used with control series and the production of SF1 class concrete with fewer admixtures is due to the smoothness surface structure of marble aggregates. Kore and Vyas [18] stated in their study that the workability properties of the marble aggregate series increased due to the smooth surface structure of the marble aggregate. As can be seen in Fig. 9b, it has been determined that the T_{500} times gradually increase with the increase in the use of marble aggregate in the series with marble aggregate. T_{500} times were found to be 1.20, 1.74, 1.82 and 1.90 *sec* for control, M25, M50 and M75 series, respectively. Since the value obtained from the M75 series is close to the 2.0 *sec* limit value, the amount of HP used in the M100 series has been slightly increased (3.5 %) compared to the M25, M50 and M75 series. Thus, both the slump flow and T_{500} values of the M100 series are placed in the desired class (SF1 and VS1). When the T_{500} times obtained from the M25, M50 and M75 series are examined, it is seen that the differences between them are very low (0.16 *sec*) and very close to each other.

In addition, if the same amount of HP is used in M100 series as in other marble aggregate series, it can be considered that the limit value of 2.0 *sec* may not be exceeded. However, in order to stay on the safe side in the study, it was decided to increase the amount of HP, and the limit value was avoided. While using 4.50 kg HP in the control series, 600 mm flow diameters were obtained, while using 4.40 kg HP in the M100 series, 610 mm flow diameters were obtained. Similarly, T_{500} times were obtained very close to each other (1.20 and 1.30 *sec*). As can be seen from these results, HSSCCs with very similar workability properties to

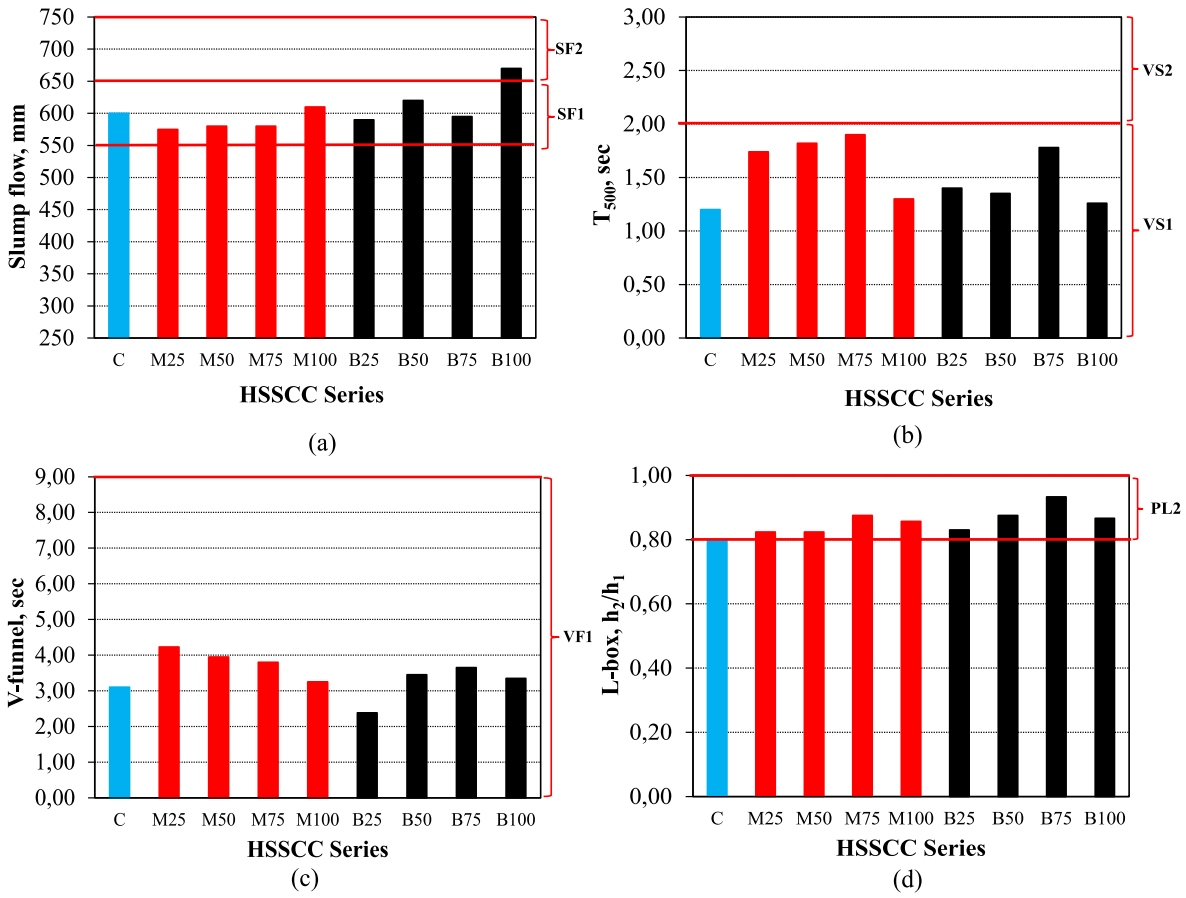

Fig. 9. Fresh concrete properties of HSCCC series a) Slump flow b) T_{500} c) V-funnel d) L-box.

control series can be produced by using less admixtures in marble aggregate series. Again, this situation is considered to be related to the smooth surface structure of the marble aggregate.

When Fig. 9c is examined, it is seen that the V funnel values obtained from the control, M25, M50, M75 and M100 series are 3.10, 4.23, 3.95, 3.80 and 3.25 *sec*, respectively. As with the T_{500} times, the V funnel values of the M25, M50 and M75 series were higher than the control series. However, there was a decrease between the M25 and M75 series. When these decrease times are examined, it is seen that they are at very low levels (0.28–0.43 *sec*). Since these values are well below 1 *sec*, they are thought to be at very close workability levels. In addition, all V funnel values obtained are well below 9 *sec*, which is the limit value of TS EN 206 + A2 [52], and it has been observed that all HSSCC series produced have a very good filling ability. In addition, conformity criteria for target values of consistence and viscosity are given in TS EN 206 + A2 [52]. These values are ± 50 mm for slump-flow diameter, ±1 *sec* for T_{500} times and ± 3 *sec* for V funnel.

As can be seen from Fig. 9d, the L-box test results varied between 0.80 and 0.93. Thus, all series are in PL2 class and have reached the ability to pass through dense reinforcements without obstruction. As stated in EFNARC [5], slump flow and V-funnel tests are performed to determine the filling ability properties of the produced self-compacting concrete, while L-box tests are performed to determine the passing ability properties. Since these tests are used to determine different properties of concrete, there is no general relationship between slump flow and V funnel test results, and L-box test results.

When the slump flow values of the basalt aggregates in Fig. 9a are examined, it is seen that the B25, B50, and B75 series are in the SF1 class and the B100 series are in the SF2 class. In the pilot castings, it was observed that the slump flow values did not remain between the limit values with the increase in basalt aggregate usage rates. It has been observed that the water requirement of HSSCC mixtures increases due to the porous structure of the basalt aggregates and the high water absorption amount. For this reason, with the increase of the B substitution in the HSSCC series, the HP amounts were also increased. Thus, all the workability properties of the HSSCC series with basalt aggregate provided the limit values given in Fig. 9.

3.2. Hardened concrete test results

3.2.1. Ultrasonic pulse velocity test results

The variation of ultrasonic pulse velocity results according to the HSSCC series is given in Fig. 10. It was observed that the ultrasonic pulse velocity values obtained from the waste marble and basalt aggregate HSSCC series ranged between 4.95 and 5.33 km/s. When Fig. 10 is examined, it is concluded that the ultrasonic pulse velocity values of waste marble and basalt aggregates, which are substituted for crushed stone aggregate, decrease with the increase in the replacement rates. Gencel et al [19] reached similar results in their study with waste marble aggregates. Ultrasonic pulse velocity values of the 28-day series, in which 100 % of the waste marble aggregate was used, decreased by 2.7 % compared to the control series. If the curing period was 180 days, the decrease rate was 3.8 %. When the HSSCC series produced with basalt aggregate were examined, the ultrasonic pulse velocity values of the 28-day series in which basalt aggregate was used at 100 % decreased by 5.2 % compared to the control series. If the curing period was 180 days, the decrease rate was 7 % compared to the control series. As the basalt and waste marble aggregate replacement ratios increased in the HSSCC series, it was evaluated that the series had a more porous structure compared to the limestone aggregate (control) series. This situation caused lower ultrasonic pulse velocity values in HSSCC series produced with waste marble and basalt aggregate.

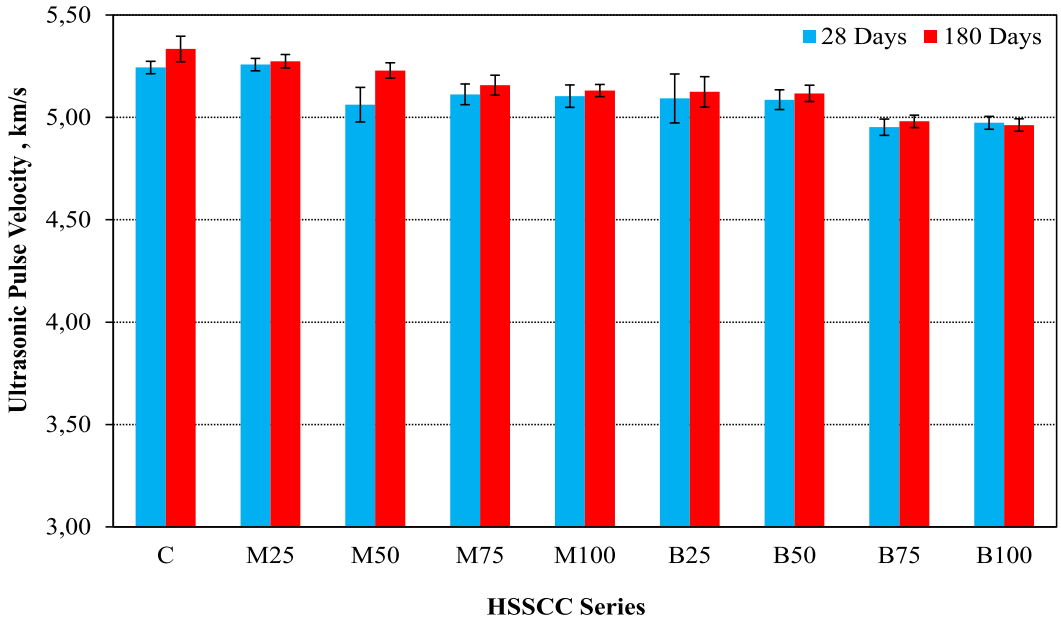

Fig. 10. Variation of ultrasonic pulse velocity results according to HSSCC series.

The specific gravity of limestone, basalt, and marble aggregates were 2.698, 2.64, and 2.55, respectively, and the water absorption values were 0.689, 1.13, and 0.692, respectively. As can be seen from the results of the obtained water absorption value, it is considered that the basalt aggregate has a more porous structure. For this reason, it is thought that lower ultrasonic pulse velocity values are obtained from the concretes produced with basalt aggregate. In the study, concrete production was carried out by replacing waste marble and basalt aggregates with limestone aggregates by volume. As can be seen from the mixing ratios given in Table 4, in case of using waste marble and basalt aggregate, concretes with lower unit weight was produced compared to the control series. It is also considered that the reason for the decrease in the ultrasonic pulse velocity with the increase in the B and M ratios in the HSSCC series may be due to the decrease in the unit weights. Gencel et al.[19] also reached similar results regarding the decrease in ultrasonic pulse velocity with the decrease in unit weights.

It was understood that with the increase of the curing times, the values also increased; that is, the HSSCC series became more impermeable. In the studies of Nik and Omran[53], it was stated that ultrasonic pulse velocities increase depending on the age of the concrete. They explained the reason for this as the disappearance of the capillary pores and cracks in the cement part of the concrete and the hydration development with the increasing age of the concrete, thus reducing the nominal resistance against the transmission of pulses.

3.2.2. Compressive strength test results

The variation of the compressive strength results according to the HSSCC series is given in Fig. 11. The compressive strengths of the waste marble and basalt aggregate series varied between 85 and 114 MPa. In the series with waste marble aggregate, after 28 days of curing, the highest compressive strength was measured in M50 with an increase of 4 % compared to the C series, while it was measured in the B100 series

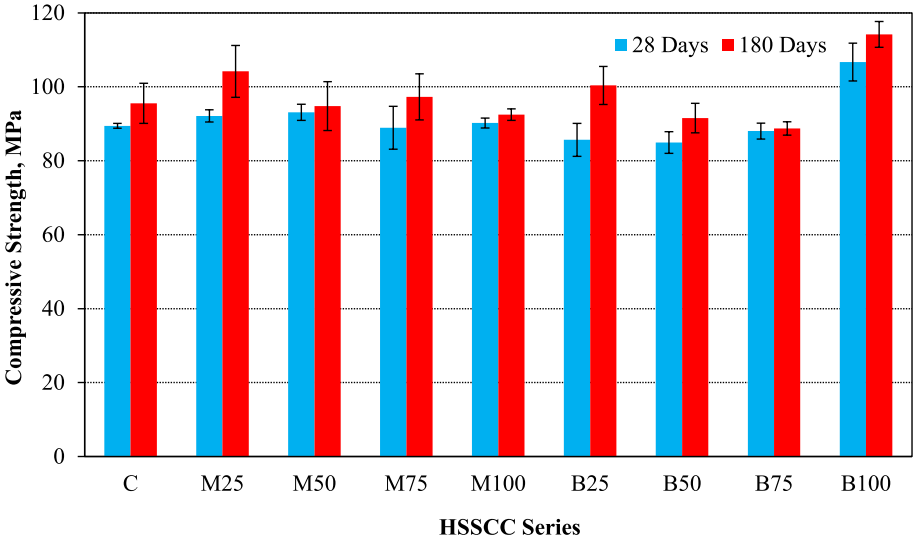

Fig. 11. Variation of compressive strength results according to HSSCC series.

with an increase of 19.2 % in the series with basalt aggregate. When 180-day curing was applied to HSSCC series, the highest compressive strengths were obtained from M25 series in case of using marble aggregate and from B100 series in case of using basalt aggregate. The compressive strength of the M25 series increased by 9.1 % compared to the C series, while the compressive strength of the B100 series increased by 19.5 %. This high increase in the B100 series can be explained by the fact that the aggregates in the concrete are composed of regular grains and the small number of voids formed under the surfaces of the irregular grains, as stated by Ostrowski[54]. Except for the series in which the basalt aggregate was replaced by 100 %, the compressive strengths were quite close to each other in the other series. The high compressive strength of basalt stone may have increased the compressive strength of HSCC series with basalt aggregate. In the compressive tests performed on 15 cm stone cubes prepared from basalt and limestone, basalt can reach a compressive strength of 150–170 MPa, and limestone can reach a compressive strength of 70–90 MPa [14]. It was determined that the compressive strengths increased with the increase in the curing times in all series. This shows that hydration reactions continue with the increase in curing times and additional C—S—H gels are formed, increasing the compressive strength of concrete. Hebhoub et al.[17], in their study where they substituted waste marble aggregates in concrete, evaluated that the reason for increasing the compressive strength of waste marble aggregate was due to the high carbonate content of the marble and the improvement of the bonds between the aggregate and cement paste.

In general, when the literature is examined, the compressive strength of concrete and building stones also increases with the increase in ultrasonic pulse velocity[55]. However, in this study, higher compressive strengths were obtained from some series with low ultrasonic pulse velocity. Ultrasonic pulse velocity results decrease with the increase in the usage rates of waste marble and basalt aggregate. It has been observed that the compressive strengths increase with the increase in ultrasonic pulse velocities in the series with marble aggregates. This situation is compatible with the literature. However, it was concluded that the relationship between ultrasonic pulse velocities and compressive strengths is not very strong. In the series with basalt aggregate, on the other hand, the compressive strengths decrease with the increase in ultrasonic pulse velocities. The obtained relationship is quite weak and incompatible with the literature. The reason for this situation is that basalt aggregates have a more porous structure as can be understood from their water absorption values. However, as can be understood from the aggregate tests, basalt aggregates are a type of aggregate with high mechanical properties, although they have a porous structure. In particular, the highest compressive strengths were obtained from the series using 100 % basalt aggregate. As a result, since the highest compressive strengths were obtained from the series with the lowest ultrasonic pulse velocities, a significant relationship could not be obtained between the ultrasonic pulse velocities and the compressive strengths in the series with basalt aggregate.

3.2.3. *Splitting-tensile strength test results*

The splitting-tensile strength results obtained from the HSSCC series are given in Fig. 12. As seen in the figure, the splitting-tensile strength results vary between 4.46 and 5.45 MPa. Experimental results show that waste marble and basalt aggregates improve the splitting-tensile strength of HSSCCs. This increase in strength may be due to the better filling effect of waste marble and basalt aggregates in the mixtures and their bonding to the cement paste. SEM images also confirm this (Section 3.2.8). Similar to compressive strengths, it was observed that with the increase in curing times, splitting-tensile strengths also increased in general. The highest strength increase rate of 18.63 % was obtained from the B50 series, in which 50 % basalt aggregate was used. When the waste marble and basalt aggregate series with a curing period of 28 days were compared, generally lower split-tensile strengths were determined in the basalt aggregate series, except for the B100 series. The highest splitting-tensile strengths obtained from the HSSCC series, in which the curing times were applied for 180 days, were obtained from the B50 and B100 series, with 5.40 and 5.45 MPa, respectively.

3.2.4. *Rapid chloride permeability test results*

The variation of the rapid chloride permeability results with respect to the HSSCC series is given in Fig. 13. The rapid chloride permeability results obtained from the HSSCC series containing waste marble and basalt aggregates ranged from 160 to 328 Coulombs. When the ASTM C 1202 [49] limit values given in Table 5 are examined, it is concluded that the rapid chloride permeability results obtained from the test specimens are very low. It is known that pozzolanic materials are used in concrete production to reduce chloride permeability of concretes, and in

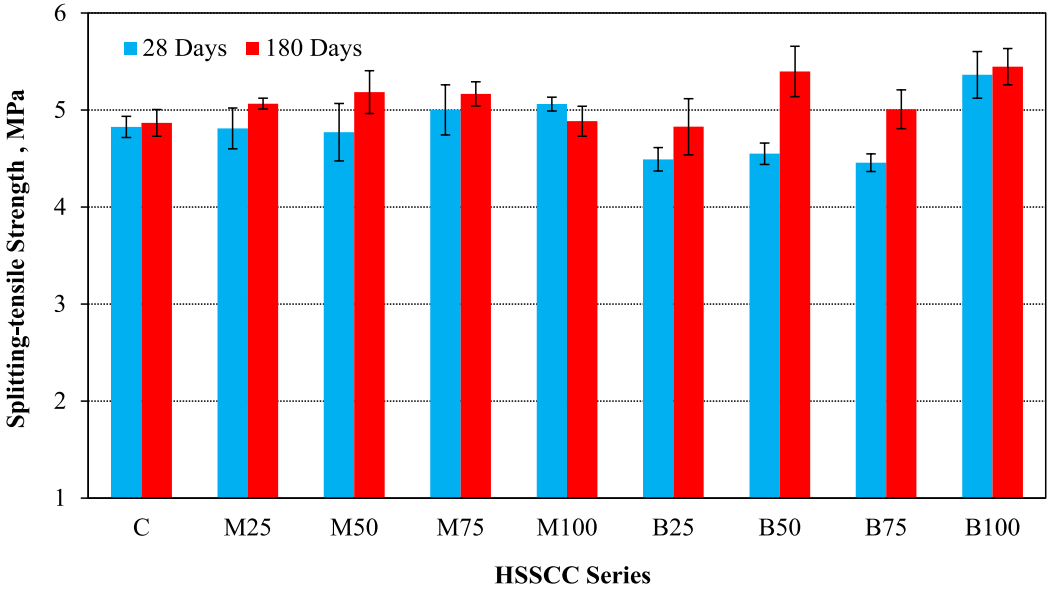

Fig. 12. Variation of splitting-tensile strength results according to HSSCC series.

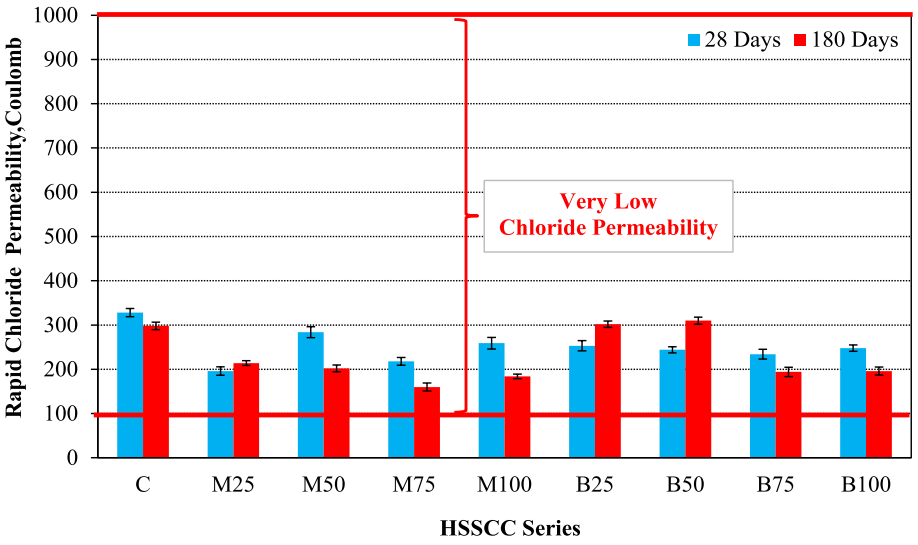

Fig. 13. Variation of rapid chloride permeability results according to HSSCC series.

this study, silica fume, a pozzolanic material, was used. With the use of silica fume, silica fume participates in pozzolanic reactions, producing secondary CSHs that lead to filling the capillary pores and thus improving the permeability of the concrete [56]. The main reason why all batches produced have very low chloride permeability levels is the use of silica fume in concrete production. From these results, it is understood that the produced concrete series will be highly resistant to corrosion if used in environments containing chloride. While the average chloride permeability obtained from the waste marble aggregate series (M0, M25, M50, M75, and M100) with a curing period of 28 days was 257 Coulombs, the average of the 180-day series was 211.6 Coulombs. In the case of basalt aggregate series (B0, B25, B50, B75, and B100) cured for 28 days, the average chloride permeability was 261.4 Coulombs, while in the case of curing for 180 days, it was 260 Coulombs. When the apparent porosity and chloride permeability results were examined, it was concluded that there was no strong relationship between them. No trend could be obtained regarding the effect of different aggregate types and usage rates on chloride permeability. When all HSSCC series were examined, it was concluded that chloride permeability generally decreased (except for M25, B25 and B50 series) with increasing curing times.

3.2.5. *Electrical resistivity test results*

The variation of the electrical resistivity results according to the HSSCC series is given in Fig. 14. The electrical resistivity values of the HSSCC series are between 46 and 57.5 kΩ.cm. Since the electrical resistivity values are>20 kΩ.cm according to Table 6, it is concluded that the produced HSSCC series are resistant to corrosion. The average of the electrical resistivity values obtained from the waste marble aggregate series (M0, M25, M50, M75, and M100) in which the curing period was applied for 28 and 180 days was obtained as 51.6 and 52.5 kΩ.cm, respectively. The mean values obtained from the basalt aggregate series (B0, B25, B50, B75, and B100) were determined as 50.74 and 51.28 kΩ.cm, respectively. When the waste marble and basalt aggregate HSSCC series were compared, higher electrical resistivity values were obtained in the waste marble aggregate series, albeit at very low rates. In general, it was observed that the electrical resistivity values increased with the increase in the curing times. With the use of silica fume admixture in the HSSCC series, the concretes became more impermeable, their electrical conductivity properties decreased and the electrical resistivity values of

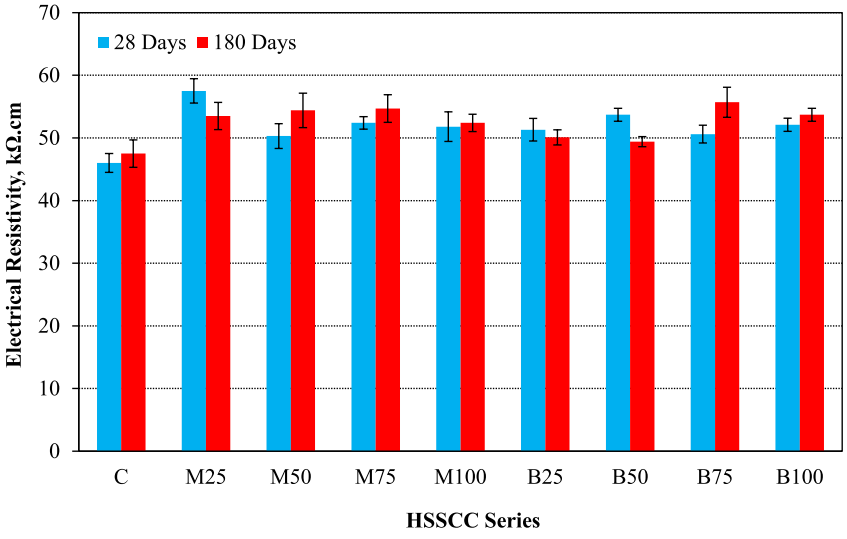

Fig. 14. Variation of electrical resistivity results according to HSSCC series.

the concretes increased.

The relationship between the electrical resistivity and rapid chloride permeability results obtained from all series is given in Fig. 15. When Fig. 15 is examined, it is concluded that there is a strong relationship between the series and that the rapid chloride permeability values decrease with the increase in the electrical resistivity values. Statistical analysis of Fig. 15 was provided at the 95 % confidence interval. As a result of the ANOVA test, the F value was 44.726 and the p-value was 0.000 (a number very close to zero). Since the p-value is less than α, the H_0 hypothesis is rejected. In other words, it can be said that the model is significant at the 95 % confidence level.

3.2.6. Apparent porosity test results

The variation of the apparent porosity values with respect to the HSSCC series is given in Fig. 16. In general, the apparent porosity values decreased with the increase of curing times. It was observed that the apparent porosity values obtained from the waste marble and basalt aggregate HSSCC series ranged from 3.34 % to 4.79 %. When Fig. 16 is examined in general, the apparent porosity values in the series with waste marble aggregate are lower than the series with basalt aggregates. When the water absorption values of the basalt aggregate are examined, it is seen that they have a higher water absorption percentage than the waste marble aggregate. Thus, it is evaluated that the basalt aggregate has a more porous structure. Therefore, the apparent porosity values in the HSSCC series with basalt aggregate were higher than the series with waste marble aggregate. Since basalt aggregate is a type of volcanic rock, it has a porous structure; however, although it has voids, it is a rather hard and high mechanical property type of aggregate. Pek[57], in one of his studies, stated that the water absorption and apparent porosity values of basalt aggregate are similarly higher than those of limestone-based aggregates and that the compressive strength is 50 % higher than that of limestone aggregate.

As can be understood from the water absorption values of basalt aggregates, they have a more porous structure than other aggregates used in the study. Therefore, lower ultrasonic pulse velocity results were obtained in HSSCCs with basalt aggregates. In addition, when the apparent porosity and ultrasonic pulse velocity results are examined together, it is seen that the series with higher apparent porosity values have lower ultrasonic pulse velocities. This is thought to be due to the porous structure of basalt aggregates.

3.2.7. Sorptivity test results

Sorptivity is a transport index to address the durability performance of concrete[58]. The variation of the sorptivity coefficient results according to the HSSCC series is shown in Fig. 17. When Fig. 17 is examined, it is seen that the sorptivity coefficient results obtained from the series vary between 0.0030 and 0.0082 mm/sn$^{0.5}$. When Fig. 17 is examined in general, lower sorptivity coefficient values were obtained in the series with waste marble aggregate, as in the apparent porosity test results. It was concluded that the increase of curing times decreased the sorptivity coefficient values in general.

Fig. 18 shows the relationships between the apparent porosity and sorptivity coefficient results obtained from all HSSCC series. As seen in Fig. 18, it was concluded that with the increase in the apparent porosity values, the sorptivity coefficient values also increased. It has been determined that there is a strong relationship between the apparent porosity and sorptivity coefficient results.

Statistical analysis of Fig. 18 was provided at the 95 % confidence interval. As a result of the ANOVA test, the F value was 85.365 and the p-value was 0.000 (a number very close to zero). Since the p-value is less than α, the H_0 hypothesis is rejected. In other words, it can be said that the model is significant at the 95 % confidence level.

3.2.8. Internal structure analysis

Internal structure image analyses of the HSSCC series M100, B100, and control (C) specimens were performed with the scanning electron microscope (SEM) at low (×1000) and high (×3000) magnifications after 180 days of curing. In addition, Energy Dispersive X-ray (EDX) analyzes were applied to the HSSCC series for which SEM analysis was performed. Accordingly, the densities of the elements in the M100 and B100 series were observed in Fig. 19, and the interface transition zones (ITZ) were determined. When Fig. 19a is examined, it is observed that the regions where the Ca element originating from the CaO in the internal structure of the waste marble aggregate in the M100 specimen are concentrated can be seen, and the density of the Si element increases in the transitions from marble aggregates to cement paste. In the B100 specimen in Fig. 19b, on the other hand, it was observed that Si and Ca elements were formed in similar amounts in the areas where cement paste was present, and the Si density increased with the presence of Si elements in the basalt structure during the transition from cement paste to basalt aggregate. These observations confirm the results of the XRF analysis given in Table 2 of Section 2.1.

SEM images obtained from C, M100, and B100 series are given in Figs. 20, 21, and 22, respectively. From the SEM images observed in Figs. 20, 21, and 22, it is seen that the dense microstructure of the cement pastes in the waste marble and basalt aggregate HSSCC series are similar to each other. Different aggregates used in concrete have varying physical and chemical properties, and this directly affects the ITZ

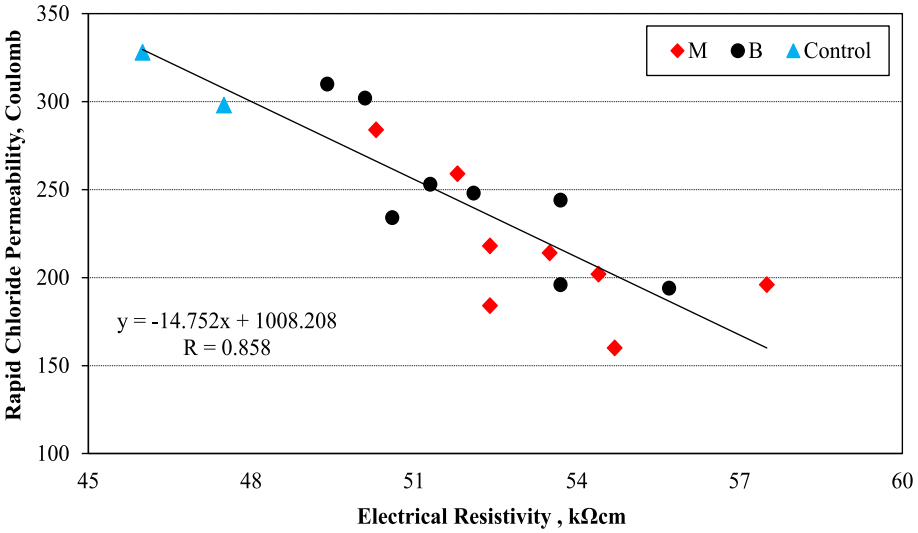

Fig. 15. Relationship between electrical resistivity and rapid chloride permeability results.

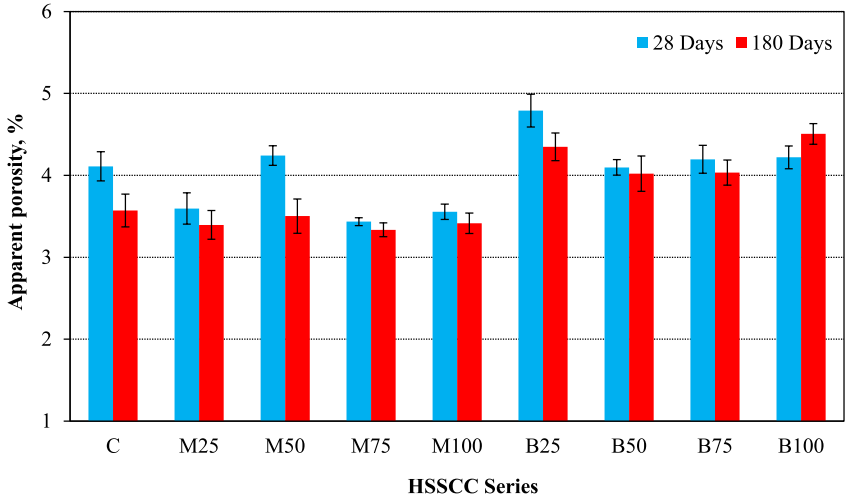

Fig. 16. Variation of apparent porosity results according to the HSSCC series.

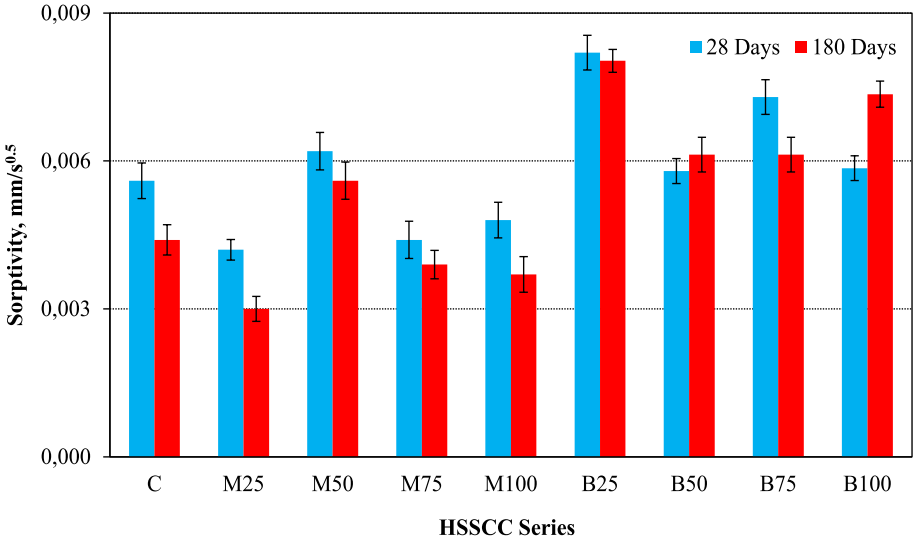

Fig. 17. Variation of sorptivity coefficient results according to HSSCC series.

properties in concrete[59]. The ITZ between cement paste and aggregate is one of the important factors affecting the mechanical properties of concrete [60,61]. When the SEM images in Fig. 21a and 22a are examined, it is observed that the micro cracks formed in the ITZ regions of the aggregates and cement paste, reducing the compressive and tensile strength of the hardened mortars, occur at narrower intervals in the B100 and M100 series, and at wider intervals in the C series seen in Fig. 20a. This situation can be evaluated as it contributes to the compressive and tensile strengths of B100 and M100 series being higher than the strength of C series.

The durability of concrete depends on the microcrack system that decides when the material will fail. Destructive processes in concrete strength can begin with microcracks in contact between coarse aggregate and cement matrix[62]. According to the compressive strength test results obtained in the study, the fact that the strength results of the B100 series, in which 100 % basalt aggregate is used, are slightly higher than the other series, can be attributed to the fact that the strength of the basalt aggregate is higher than that of limestone and waste marble aggregates. Similarly, Li et al[63]; They evaluated that the intrinsic strength of coarse basalt aggregate is higher than that of conventional coarse aggregates, the use of dense basalt aggregate can improve the compressive strength of concrete, and the ITZ between coarse basalt aggregate and cement paste can become stronger by optimizing the powder content in the mixture. This situation can also be observed from the SEM images in Fig. 19b and Fig. 22b.

The use of a high percentage of waste marble aggregate in the HSSCC series generally increased the splitting tensile strengths. This situation can be evaluated as the ITZ in the M100 series has low porosity and good bonding structure, as can be seen from the internal structure analyzes in Fig. 19a and Fig. 21b. Vardhan et al.[64], stated that the addition of waste marble to the mixtures would not have much effect on the hydration of cement, and C—S—Hs will spread better. Thus, the C—S—H gels and C-Hs in the HSSCC series remain almost the same in all series.

In the SEM and EDX analyses, it was observed that there was a strong bond between the aggregate particles in the waste marble and basalt aggregate HSSCC series and the cement paste. Especially from the SEM images of M100 (Fig. 19a and Fig. 21b), the absence of a boundary line between the aggregate and the cement paste indicates a strong bond between them.

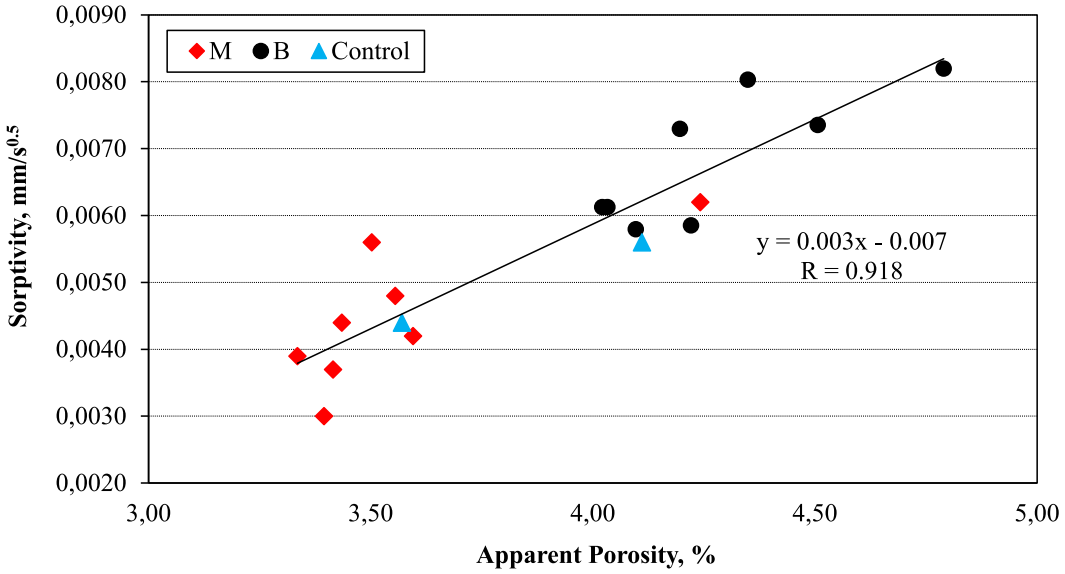

Fig. 18. Relationship between apparent porosity and sorptivity coefficient results.

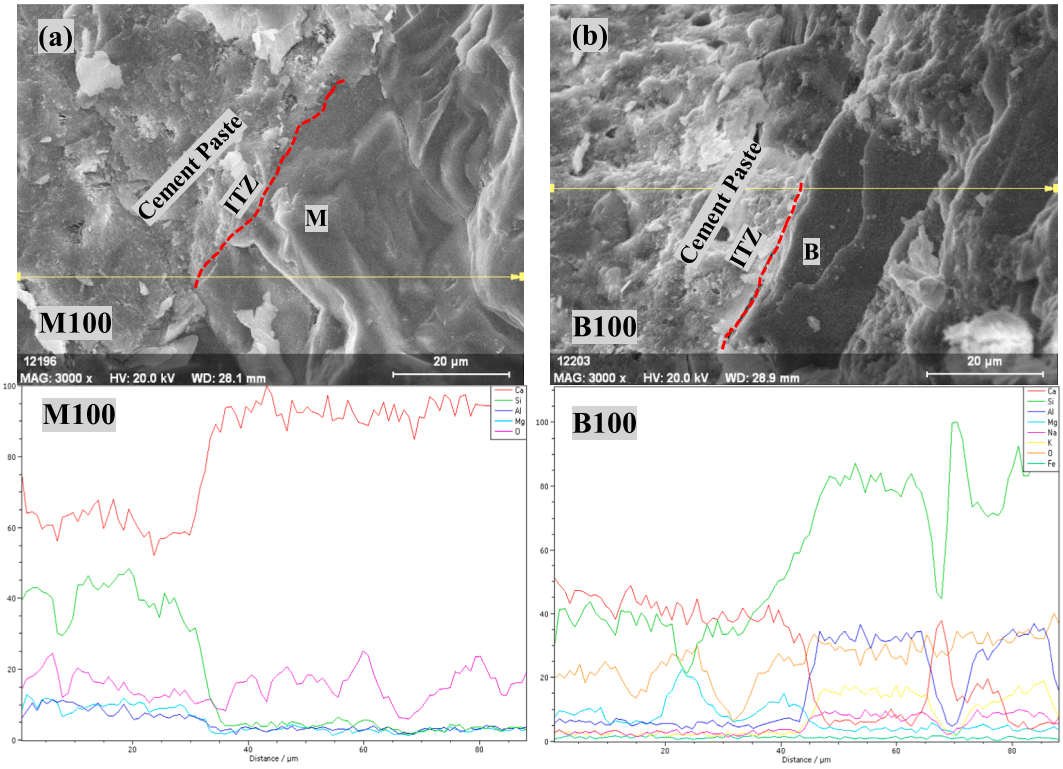

Fig. 19. SEM - EDX analysis a) M100 b) B100.

4. Results and discussion

All conclusions obtained from the study are based on a specific study using the specific tested materials and under the specific research conditions, and many cannot be generalized. According to the results obtained from the tests;

- The study's results showed that basalt or waste marble aggregates could be useful in developing HSSCC. In addition, it is evaluated that using waste marbles as coarse aggregate in SCCs will reduce production costs and contribute to environmental waste management.
- According to the fresh concrete test results, segregation was not observed in all HSSCC series with basalt, and waste marble aggregate, and the limit values given in TS EN 206 + A2 were met.
- With the increase in curing times, the ultrasonic pulse velocity values also increased, and HSSCC series became more impermeable.
- The highest compressive strength values of the HSSCC series were obtained from the B100 series, which were cured for 180 days. This

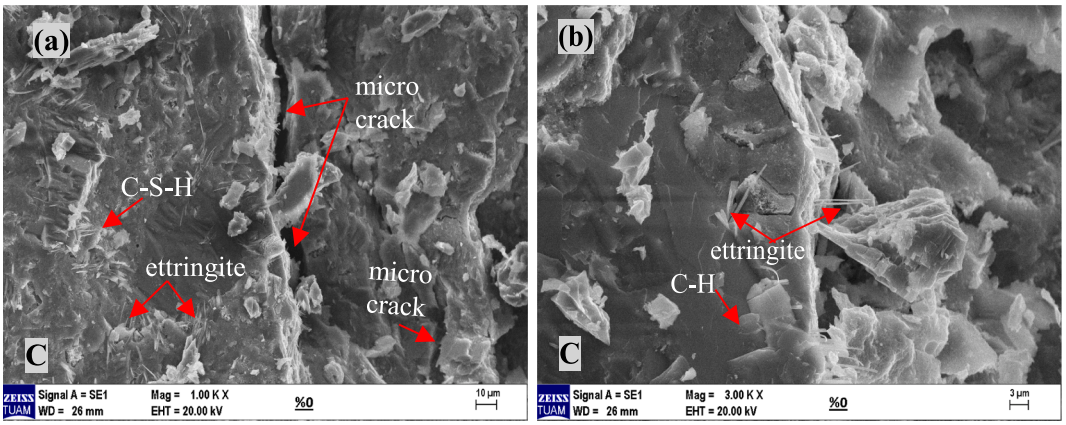

Fig. 20. SEM images of Control (C) series a) × 1000b) × 3000 magnification.

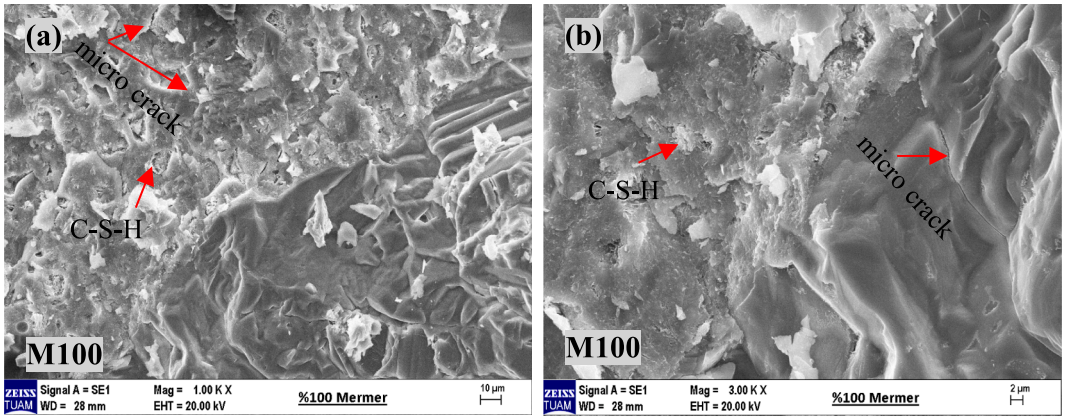

Fig. 21. SEM images of M100 series a) × 1000b) × 3000 magnification.

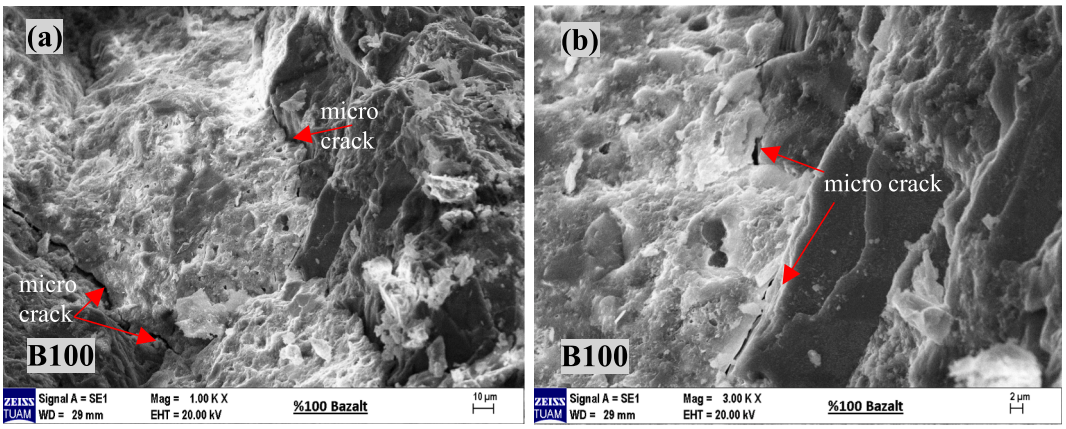

Fig. 22. SEM images of B100 series a) × 1000b) × 3000 magnification.

result was evaluated as the intrinsic strength of basalt aggregate is higher than limestone and waste marble aggregates, it consists of regular grains and good bonding between aggregate and paste. The compressive strength results of other HSSCC series were very close to each other.

- Similar to compressive strengths, with the increase in curing times, splitting-tensile strengths also increased in general. The highest value was obtained from the B100 series, in which basalt aggregate was used at 100 %, as in the compressive strength.
- All HSSCC series have very low chloride permeability. In addition, in terms of electrical resistivity measurements of all series, it has been concluded that HSSCC series are highly resistant to corrosion when used in environments containing chloride.
- When the apparent porosity and sorptivity coefficient values are examined in general, the apparent porosity and sorptivity coefficient values of the waste marble aggregate series are lower than the basalt aggregated series.
- From the SEM and EDX analyses, it was determined that the waste marble and basalt aggregates intensified the binder-aggregate interface in the HSSCC series and formed a strong bond in general.

CRediT authorship contribution statement

Ahmet Raif Boğa: Conceptualization, Methodology, Formal analysis, Investigation, Writing – original draft, Writing – review & editing, Supervision. **Ahmet Ferdi Şenol:** Conceptualization, Methodology, Formal analysis, Investigation, Writing – original draft, Writing – review & editing, Visualization.

Declaration of Competing Interest

The authors declare that they have no known competing financial interests or personal relationships that could have appeared to influence the work reported in this paper.

Data availability

Data will be made available on request.

References

[1] X.X. Zhang, G. Ruiz, R.C. Yu, M. Tarifa, Fracture behaviour of high-strength concrete at a wide range of loading rates, Int. J. Impact Eng 36 (10–11) (Oct. 2009) 1204–1209, https://doi.org/10.1016/J.IJIMPENG.2009.04.007.

[2] V.K.R. Kodur, T.C. Wang, F.P. Cheng, Predicting the fire resistance behaviour of high strength concrete columns, Cem. Concr. Compos. 26 (2) (2004) pp, https://doi.org/10.1016/S0958-9465(03)00089-1.

[3] O.E. Babalola, P.O. Awoyera, D.H. Le, L.M. Bendezú Romero, A review of residual strength properties of normal and high strength concrete exposed to elevated temperatures: Impact of materials modification on behaviour of concrete composite, Constr. Build. Mater. 296 (2021), https://doi.org/10.1016/j.conbuildmat.2021.123448.

[4] H. Okamura ve, M. Ouchi, Self-compacting concrete, J. Adv. Concr. Technol. (2003) 5–15.

[5] *EFNARC, "The European Guidelines for Self-Compacting Concrete.* The European Guidelines for Self Compacting Concrete, 2005.

[6] A. Raif Boğa, C. Karakurt, A. Ferdi Şenol, The effect of elevated temperature on the properties of SCC's produced with different types of fibers, Constr. Build. Mater. 340 (Jul. 2022), 127803, https://doi.org/10.1016/J.CONBUILDMAT.2022.127803.

[7] S.S. Vivek, G. Dhinakaran, Fresh and hardened properties of binary blend high strength self compacting concrete, Eng. Sci. Technol. an Int. J. 20 (3) (2017) pp, https://doi.org/10.1016/j.jestch.2017.05.003.

[8] M.S. Nadesan, P. Dinakar, Permeation properties of high strength self-compacting and vibrated concretes, J. Build. Eng. 12 (2017), https://doi.org/10.1016/j.jobe.2017.06.003.

[9] M. Soleymani Ashtiani, A.N. Scott, R.P. Dhakal, Mechanical and fresh properties of high-strength self-compacting concrete containing class C fly ash, Constr. Build. Mater. 47 (Oct. 2013) 1217–1224, https://doi.org/10.1016/J.CONBUILDMAT.2013.06.015.

[10] N. Arabi, H. Meftah, H. Amara, O. Kebaïli, L. Berredjem, Valorization of recycled materials in development of self-compacting concrete: Mixing recycled concrete aggregates – Windshield waste glass aggregates, Constr. Build. Mater. 209 (2019), https://doi.org/10.1016/j.conbuildmat.2019.03.024.

[11] C. Agasnalli, H.C. Hema, T. Lakkundi, K.D. Chandrappa, Integrated assessment of granite and basalt rocks as building materials, Mater. Today:. Proc. 62 (Jan. 2022) 5388–5391, https://doi.org/10.1016/J.MATPR.2022.03.546.

[12] A. Ibrahim, S. Faisal, N. Jamil, Use of basalt in asphalt concrete mixes, Constr. Build. Mater. 23 (1) (2009) pp, https://doi.org/10.1016/j.conbuildmat.2007.10.026.

[13] S. K. I, M. L, M. P. C, and H. K. B, 'Experimental Study on the Use of Basalt Aggregate in Concrete Mixes', *Int. J. Civ. Eng.*, vol. 2, no. 4, 2015, doi: 10.14445/23488352/ijce-v2i4p107.

[14] M. Sarireh, Testing the Properties of Concrete Using Natural and Local Aggregates, J. Mech. Civ. Eng. 19 (2022) 65–75.

[15] B. Worku Yifru and B. Bewket Mitikie, 'Partial replacement of sand with marble waste and scoria for normal strength concrete production', 123AD, doi: 10.1007/s42452-020-03716-9.

[16] *Natural Stones Industry Report.* Ankara: Directorate, Export General, Metal Mining, and Forest Products Department, Ministry of Commerce of the Republic of Turkey, 2021.

[17] H. Hebhoub, H. Aoun, M. Belachia, H. Houari, E. Ghorbel, Use of waste marble aggregates in concrete, Constr. Build. Mater. 25 (3) (Mar. 2011) 1167–1171, https://doi.org/10.1016/J.CONBUILDMAT.2010.09.037.

[18] S.D. Kore, A.K. Vyas, Impact of marble waste as coarse aggregate on properties of lean cement concrete, Case Stud. Constr. Mater. 4 (2016), https://doi.org/10.1016/j.cscm.2016.01.002.

[19] O. Gencel, C. Ozel, F. Koksal, E. Erdogmus, G. Martínez-Barrera, W. Brostow, Properties of concrete paving blocks made with waste marble, J. Clean. Prod. 21 (1) (Jan. 2012) 62–70, https://doi.org/10.1016/J.JCLEPRO.2011.08.023.

[20] S. A. Mangi *et al.*, 'Recycling of ceramic tiles waste and marble waste in sustainable production of concrete: a review', vol. 1, p. 3, doi: 10.1007/s11356-021-18105-x.

[21] M. Tennich, A. Kallel, M. Ben Ouezdou, Incorporation of fillers from marble and tile wastes in the composition of self-compacting concretes, Constr. Build. Mater. 91 (2015), https://doi.org/10.1016/j.conbuildmat.2015.04.052.

[22] V. Corinaldesi, G. Moriconi, T.R. Naik, Characterization of marble powder for its use in mortar and concrete, Constr. Build. Mater. 24 (1) (2010) pp, https://doi.org/10.1016/j.conbuildmat.2009.08.013.

[23] M. Singh, K. Choudhary, A. Srivastava, K. Singh Sangwan, D. Bhunia, 'A study on environmental and economic impacts of using waste marble powder in concrete, J. Build. Eng. 13 (2017), https://doi.org/10.1016/j.jobe.2017.07.009.

[24] A.A. Aliabdo, A.E.M. Abd Elmoaty, E.M. Auda, Re-use of waste marble dust in the production of cement and concrete, Constr. Build. Mater. 50 (Jan. 2014) 28–41, https://doi.org/10.1016/J.CONBUILDMAT.2013.09.005.

[25] M.A. Rashwan, T.M. Al Basiony, A.O. Mashaly, M.M. Khalil, Self-compacting concrete between workability performance and engineering properties using natural stone wastes, Constr. Build. Mater. 319 (Feb. 2022), 126132, https://doi.org/10.1016/J.CONBUILDMAT.2021.126132.

[26] A. Talah, F. Kharchi, R. Chaid, Influence of Marble Powder on High Performance Concrete Behavior, Procedia Eng. 114 (2015), https://doi.org/10.1016/j.proeng.2015.08.010.

[27] C. Vaidevi, T. Felix Kala, A.R.R. Kalaiyarrasi, Mechanical and durability properties of self-compacting concrete with marble fine aggregate, Mater. Today:. Proc. 22 (Jan. 2020) 829–835, https://doi.org/10.1016/J.MATPR.2019.11.019.

[28] D.M. Sadek, M.M. El-Attar, H.A. Ali, Reusing of marble and granite powders in self-compacting concrete for sustainable development, J. Clean. Prod. 121 (2016), https://doi.org/10.1016/j.jclepro.2016.02.044.

[29] A. André, J. De Brito, A. Rosa, D. Pedro, Durability performance of concrete incorporating coarse aggregates from marble industry waste, J. Clean. Prod. 65 (Feb. 2014) 389–396, https://doi.org/10.1016/J.JCLEPRO.2013.09.037.

[30] R. Choudhary, R. Gupta, R. Nagar, Impact on fresh, mechanical, and microstructural properties of high strength self-compacting concrete by marble cutting slurry waste, fly ash, and silica fume, Constr. Build. Mater. 239 (Apr. 2020), 117888, https://doi.org/10.1016/J.CONBUILDMAT.2019.117888.

[31] G. Srikanth, M. Safiuddin, M. Mustafeezul Haque, M. Rizwan, Study on mechanical properties of concrete using different types of coarse aggregates, Mater. Today:. Proc., Jun. (2022), https://doi.org/10.1016/J.MATPR.2022.06.033.

[32] T. Uygunoğlu, I.B. Topçu, A.G. Çelik, Use of waste marble and recycled aggregates in self-compacting concrete for environmental sustainability, J. Clean. Prod. 84 (1) (Dec. 2014) 691–700, https://doi.org/10.1016/J.JCLEPRO.2014.06.019.

[33] Turkish Standards Institute, TS EN 197–1, Cement-Stage 1: General Cements-Component, Ankara, Turkey, 2012.

[34] Turkish Standards Institute, TS EN 1097-2, Tests for mechanical and physical properties of aggregates - Part 2:Methods for the determination of resistance to fragmentation, Ankara, Turkey (2020).

[35] BS 812–112. Testing aggregates. Method for determination of aggregate impact value (AIV), British Standarts Institution. 1990.

[36] BS 812-110. Testing Aggregates–Part 110: Methods for Determination of Aggregate Crushing Value (ACV), British Standarts Institution, 1990.

[37] Turkish Standards Institute. TS EN 1926, Natural stone test methods - Determination of uniaxial compressive strength. Ankara. 2007.

[38] M. Kamani, R. Ajalloeian, Investigation of the changes in aggregate morphology during different aggregate abrasion/degradation tests using image analysis, Constr. Build. Mater. 314 (Jan. 2022), 125614, https://doi.org/10.1016/J.CONBUILDMAT.2021.125614.

[39] R. Zhang, T.S. Qureshi, D.K. Panesar, Use of industrial waste in construction and a cost analysis, in: In *Handbook of SustaInable Concrete and Industrial Waste Management*, 2022, pp. 615–635.

[40] Turkish Standards Institute, TS 802, Design of concrete mixes, Ankara, 2016.

[41] Turkish Standards Institute, TS EN 12350–8, Testing Fresh Concrete - Part 8: Self-Compacting Concrete - Slump-Flow Test, Ankara, Turkey, 2019.

[42] Turkish Standards Institute, TS EN 12350–9, Testing Fresh Concrete - Part 9: Self-Compacting Concrete - V-funnel Test, Ankara, Turkey, 2011.

[43] Turkish Standards Institute, TS EN 12350–10, Testing Fresh Concrete - Part 10: Self-Compacting Concrete - L-box Test, Ankara, Turkey, 2011.

[44] Turkish Standards Institute, TS EN 12390–1, Testing hardened concrete - Part 1: Shape, dimensions and other requirements for specimens and moulds, Ankara, Turkey, 2021.

[45] Turkish Standards Institute, TS EN 12390–2, Testing hardened concrete - Part 2: Making and curing specimens for strength tests, Ankara, Turkey, 2019.

[46] Turkish Standards Institute, TS EN 12504–4, Testing Concrete in Structures - Part 4: Determination of Ultrasonic Pulse Velocity, Ankara, Turkey, 2021.

[47] Turkish Standards Institute, TS EN 12390–3, Testing Hardened Concrete - Part 3: Compressive Strength of Test Specimens, Ankara, Turkey, 2019.

[48] Turkish Standards Institute, TS EN 12390–6, Testing Hardened Concrete - Part 6: Tensile Splitting Strength of Test Specimens, Ankara, Turkey, 2010.

[49] ASTM C1202–19 , Standard Test Method for Electrical Indication of Concrete's Ability to Resist Chloride Ion Penetration , ASTM International 2019 , West Conshohocken, PA, USA.

[50] H. W. Song and V. Saraswathy, 'Corrosion monitoring of reinforced concrete structures - A review', *Int. J. Electrochem. Sci.*, vol. 2, no. 1, 2007.

[51] I. Türkmen, A. Kantarci, Effects of expanded perlite aggregate and different curing conditions on the physical and mechanical properties of self-compacting concrete, Build. Environ. 42 (6) (Jun. 2007) 2378–2383, https://doi.org/10.1016/J.BUILDENV.2006.06.002.

[52] *Turkish Standards Institute.TS EN 206+A2, Concrete - Specification, performance, production and conformity. Ankara.* Turkey, 2021.
[53] A. Sadeghi Nik and O. Lotfi Omran, 'Estimation of compressive strength of self-compacted concrete with fibers consisting nano-SiO2 using ultrasonic pulse velocity', *Constr. Build. Mater.*, vol. 44, pp. 654–662, Jul. 2013, doi: 10.1016/J.CONBUILDMAT.2013.03.082.
[54] K. Ostrowski, The influence of coarse aggregate shape on the properties of high-performance, self-compacting concrete, Technical Transactions 114 (5) (2017) 25–33, https://doi.org/10.4467/2353737XCT.17.066.6423.
[55] A.A.E. Aliabdo, A.E.M.A. Elmoaty, Reliability of using nondestructive tests to estimate compressive strength of building stones and bricks, Alexandria Eng. J. 51 (3) (Sep. 2012) 193–203, https://doi.org/10.1016/J.AEJ.2012.05.004.
[56] A. Habibi, A.M. Ramezanianpour, M. Mahdikhani, O. Bamshad, RSM-based evaluation of mechanical and durability properties of recycled aggregate concrete containing GGBFS and silica fume, Constr. Build. Mater. 270 (Feb. 2021), 121431, https://doi.org/10.1016/J.CONBUILDMAT.2020.121431.
[57] N.A. Pek, Use of Basalt Aggregate in Concrete Marine Structures, Tech. J. 25 (3) (Apr. 2014) 6849–6866.
[58] Y.A. Villagrán-Zaccardi, et al., Relationship between sorptivity coefficients of concrete as calculated from the evolution of water uptake versus t0.5 or t0.25, Constr. Build. Mater. 342 (Aug. 2022), 128084, https://doi.org/10.1016/J.CONBUILDMAT.2022.128084.
[59] R. Chen, K.H. Mo, T.C. Ling, Offsetting strength loss in concrete via ITZ enhancement: From the perspective of utilizing new alternative aggregate, Cem. Concr. Compos. 127 (Mar. 2022), 104385, https://doi.org/10.1016/J.CEMCONCOMP.2021.104385.
[60] S.M. Mousavi, M.M. Ranjbar, Experimental study of the effect of silica fume and coarse aggregate type on the fracture characteristics of high-strength concrete, Eng. Fract. Mech. 258 (2021), https://doi.org/10.1016/j.engfracmech.2021.108094.
[61] L. Hong, X. Gu, F. Lin, Influence of aggregate surface roughness on mechanical properties of interface and concrete, Constr. Build. Mater. 65 (2014), https://doi.org/10.1016/j.conbuildmat.2014.04.131.
[62] G.L. Golewski, An assessment of microcracks in the Interfacial Transition Zone of durable concrete composites with fly ash additives, Compos. Struct. 200 (2018), https://doi.org/10.1016/j.compstruct.2018.05.144.
[63] P.P. Li, Q.L. Yu, H.J.H. Brouwers, Effect of coarse basalt aggregates on the properties of Ultra-high Performance Concrete (UHPC), Constr. Build. Mater. 170 (May 2018) 649–659, https://doi.org/10.1016/J.CONBUILDMAT.2018.03.109.
[64] K. Vardhan, R. Siddique, S. Goyal, Strength, permeation and micro-structural characteristics of concrete incorporating waste marble, Constr. Build. Mater. 203 (2019), https://doi.org/10.1016/j.conbuildmat.2019.01.079.